



Reduction of abnormal blood flow in frozen shoulder after shoulder manipulation under ultrasound-guided cervical nerve root block: semiquantitative analysis using dynamic magnetic resonance imaging



Yuki Iijima, MD^{a,*}, Hideharu Sugimoto, MD^b, Hideyuki Sasanuma, MD^c,
Tomohiro Saito, MD^c, Wataru Kurashina, RPT^d, Yuji Kanaya, MD^a, Katsushi Takeshita, MD^a

^aJichi Medical University, Department of Orthopaedic Surgery, Shimotsuke, Tochigi, Japan

^bShin-Kaminokawa Hospital, Department of Radiology, Kawachi, Tochigi, Japan

^cTochigi Medical Center Shimotsuga, Department of Orthopaedic Surgery, Ohira, Tochigi, Japan

^dTochigi Medical Center Shimotsuga, Department of Rehabilitation, Ohira, Tochigi, Japan

ARTICLE INFO

Keywords:

Frozen shoulder
Dynamic MRI
Manipulation
Burning sign
Abnormal blood flow
Semiquantitative diagnosis

Level of evidence: Level IV; Case Series;
Treatment Study

Background: We previously reported a characteristic dynamic magnetic resonance imaging (MRI) change in patients with frozen shoulder (FS) and named this abnormal blood flow pattern the “burning sign”. In this study, a semiquantitative method was used to evaluate changes in this abnormal blood flow pattern on dynamic MRI after shoulder manipulation under ultrasound-guided cervical nerve root block (MUC) in patients with FS.

Methods: Nineteen patients with FS underwent MUC, with dynamic MRI performed before and after. We used dynamic MRI to semiquantitatively assess changes in the burning sign at the axillary pouch (AP) and rotator interval (RI) by examining the enhancement rate in the signal intensity and the enhancement velocity. Functional assessments included a numeric rating scale score, the range of shoulder motion, the American Shoulder and Elbow Surgeons score, and the Constant score.

Results: The burning sign in the AP and RI was observed with dynamic MRI in all patients before MUC. The average interval from MUC until dynamic MRI was 8.2 months (range, 6–12). Clinical results for all patients improved after MUC. The before and after MUC enhancement rates (%) were 217 ± 51 and 85 ± 36 in the AP and 233 ± 61 and 73 ± 40 in the RI, respectively (both $P < .001$). The before and after MUC enhancement velocities (ms/s) were 902 ± 335 and 203 ± 125 in the AP and 1249 ± 634 and 213 ± 146 in the RI, respectively (both $P < .001$).

Conclusion: Dynamic MRI semiquantitatively demonstrated a reduction in abnormal blood flow and improvement in clinical results after MUC in patients with FS.

© 2022 The Authors. Published by Elsevier Inc. on behalf of American Shoulder and Elbow Surgeons. This is an open access article under the CC BY-NC-ND license (<http://creativecommons.org/licenses/by-nc-nd/4.0/>).

Frozen shoulder (FS) is a common disease characterized by limited range of motion (ROM) of the glenohumeral joint and severe shoulder pain. This condition was first described by Codman in 1934,⁵ and the prevalence of FS is reported to be 2%–5% of the total population.^{6,8} Although the clinical symptoms are relatively easy to appreciate, the ability to diagnose this disease based on imaging characteristics is considered poor. We previously found a characteristic change on dynamic 3-dimensional magnetic resonance imaging (3D MRI) in patients with

idiopathic severe FS, which we termed the “burning sign”.¹⁷ The burning sign represents an abnormally high blood flow from the acromial arterial network and the branches of the humeral circumflex arteries into the axillary pouch (AP) and the rotator interval (RI).

There are many conservative treatment options for FS including complete rest, medication, local steroid injection, physiotherapy, and hydrodistension.^{9,13,14,22} If these are not effective, then more invasive procedures are necessary, including manipulation under general anesthesia or arthroscopic capsular release.^{1,4,7} Recent studies have described shoulder manipulation under ultrasound-guided cervical nerve root block (MUC) as a treatment for FS.² We have previously described the effective and safe use of MUC over the short term.^{15,18} We also previously reported articular MRI findings after MUC and the disappearance of

This study was approved by the Jichi Medical University Institutional Review Board (A13-113)

*Corresponding author: Yuki Iijima, MD, Jichi Medical University, Department of Orthopaedic Surgery, 3311-1 Yakushiji, Shimotsuke, Tochigi 3292740822, Japan.

E-mail addresses: y-jima@omiya.jichi.ac.jp, jichi.yuki@gmail.com (Y. Iijima).

<https://doi.org/10.1016/j.jseint.2021.12.007>

2666-6383/© 2022 The Authors. Published by Elsevier Inc. on behalf of American Shoulder and Elbow Surgeons. This is an open access article under the CC BY-NC-ND license (<http://creativecommons.org/licenses/by-nc-nd/4.0/>).

iatrogenic capsular tears, bone bruises, and labral tears six months later as observed by plain MRI.¹⁶

To our knowledge, a change in the abnormal blood flow that is characteristic of FS after MUC has not yet been reported. In the field of breast cancer diagnosis, dynamic MRI has been used to distinguish malignant breast cancer from benign lesions by evaluating the slope of the washout curve of the lesion and evaluating the kinetic curve quantitatively.^{10,23} We partially referred to these methods when using dynamic MRI to evaluate changes in FS after MUC.

The purpose of this study was to use dynamic MRI to semi-quantitatively assess the reduction in abnormal blood flow after MUC in patients with FS.

Methods

Patients

This study was approved by the Jichi Medical University Institutional Review Board (A13-113). We retrospectively reviewed patients' records and MRI images. Between January 2015 and January 2017, MUC was performed for thirty-four patients in diagnosis of idiopathic FS. In this study, 19 patients who could undergo nonenhanced and dynamic enhanced MRI of the shoulder joint before and after MUC were recruited. The average age was 55.3 (range, 41–67) years, and there were 16 women and three men. Patients were diagnosed with idiopathic FS if they had limited ROM in all directions ($\leq 100^\circ$ in forward flexion [FF], $\leq 0^\circ$ in external rotation at the side [ER], and internal rotation [IR] ≤ 15) and did not respond to a combination of intra-articular steroid injections and physical therapy administered for at least 3 months. The mean time from the onset of shoulder pain to MUC was 5.2 (range, 3–12) months. Before the procedure, all patients underwent radiography of the affected shoulder in addition to dynamic MRI to exclude other shoulder-related diseases. Patients who had any of the following were excluded: rotator cuff tear, shoulder osteoarthritis, rheumatoid arthritis, calcified tendinitis, history of shoulder joint fracture, history of shoulder joint surgery, long head biceps tendon injury, diabetic stiff shoulder, or cervical spine disease.

MRI examination

All patients underwent enhanced dynamic MRI (Skyra; Siemens Medical Systems, Erlangen, Germany) preoperatively and postoperatively. Postoperative MRI was performed greater than 6 months after MUC. Before the dynamic MRI series was performed, our routine series of nonenhanced MRI was performed. After a bolus intravenous injection of the gadolinium-chelated contrast material, 3D fast low-angle shot images (repetition time, 3.1 ms; echo time, 1.26 ms) were obtained in the oblique coronal plane every 9 seconds for a total period of 3 minutes. During the final phase, we obtained four T1-weighted images at each slice level (in-phase T1-weighted image, opposed phase image, water-only image [fat suppression image], and fat-only image). All the images were recovered from a digital database.¹⁷

Semiquantitative measurement in dynamic MRI

Two shoulder surgeons (Y.I. and H.S.) and one radiologist (H.S.), each with more than 15 years' experience, independently evaluated the presence or absence of the burning sign at the AP and RI before MUC with 3D dynamic MRI. When there was disagreement over the

diagnosis, the final diagnosis was determined based on consensus. If the burning sign was noted, we assessed the burning sign at the AP and RI semiquantitatively by measuring the T1 signal intensity (SI) on dynamic MRI.

As assessment items, the enhancement rate of the SI and the enhancement velocity were measured at the AP and RI. Setting a 0.3-cm² region of interest (ROI) in the area of AP and RI on the contrast-enhanced T1-weighted image, the dynamic MRI kinetic curve of the enhancement was showed graphically (Fig. 1, Fig. 2). The enhancement rate was calculated as per the following enhancement formula:

$$\text{enhancement rate} = [(SI \text{ post} - SI \text{ pre}) / SI \text{ pre}] \times 100 (\%)$$

Because comparison of absolute values of T1 between cases is not appropriate, we elected to assess the enhancement rate of the T1 value instead; this was, therefore, a semiquantitative rather than fully quantitative analysis. These tasks were performed using a PACS workstation (SYNAPSE-Fujifilm, Tokyo, Japan) by a single shoulder surgeon (Y.I.). Mean values were determined after three measurements were performed.

Clinical evaluation

Clinical evaluations were recorded at the point of the initial and second dynamic MRI. The items assessed were a numeric rating scale (NRS) at motion, active shoulder ROM (FF, ER, and IR), the American Shoulder and Elbow Surgeons (ASES) score, and the Constant score.

Surgical procedures

Procedures were performed by two shoulder surgeons (Y.I. and H.S.) in an outpatient setting. The cervical nerve roots (C5–C6) were identified using ultrasonographic examination (Noblus; Hitachi ALOKA Medical, Tokyo, Japan); then, injection of 10 mL of 0.75% ropivacaine and 10 mL of 1% lidocaine was performed around them. Manipulation was first performed by moving the shoulder into 90° of abduction with gradual ER. After 90° of abduction and 90° of ER were obtained, the arm was maximally abducted until the patient's upper arm touched his or her ear. Progression to maximum adduction was then performed, followed by IR while in maximum adduction. Progression to maximum ER with the arm at the patient's side was followed by progression to maximum ER with the patient's arm at 45° of abduction. Finally, IR was performed until the vertebral height that could be reached by the dominant thumb was equal to that of the nondominant thumb.¹⁵

After MUC, vital signs and the swelling of the cervical block site 1 hour after anesthesia were measured for all patients to rule out pneumothorax or vascular injury. We also performed radiography and ultrasonography to detect humeral fractures, shoulder dislocations, or rotator cuff tears.

Postoperative treatment

All patients underwent a standard rehabilitation protocol including shoulder passive and active ROM exercises and stretching of the periscapular muscles by a physical therapist the day after the procedure. They continued to receive rehabilitation under the supervision of a physical therapist for 3 months. All patients successfully completed this program.

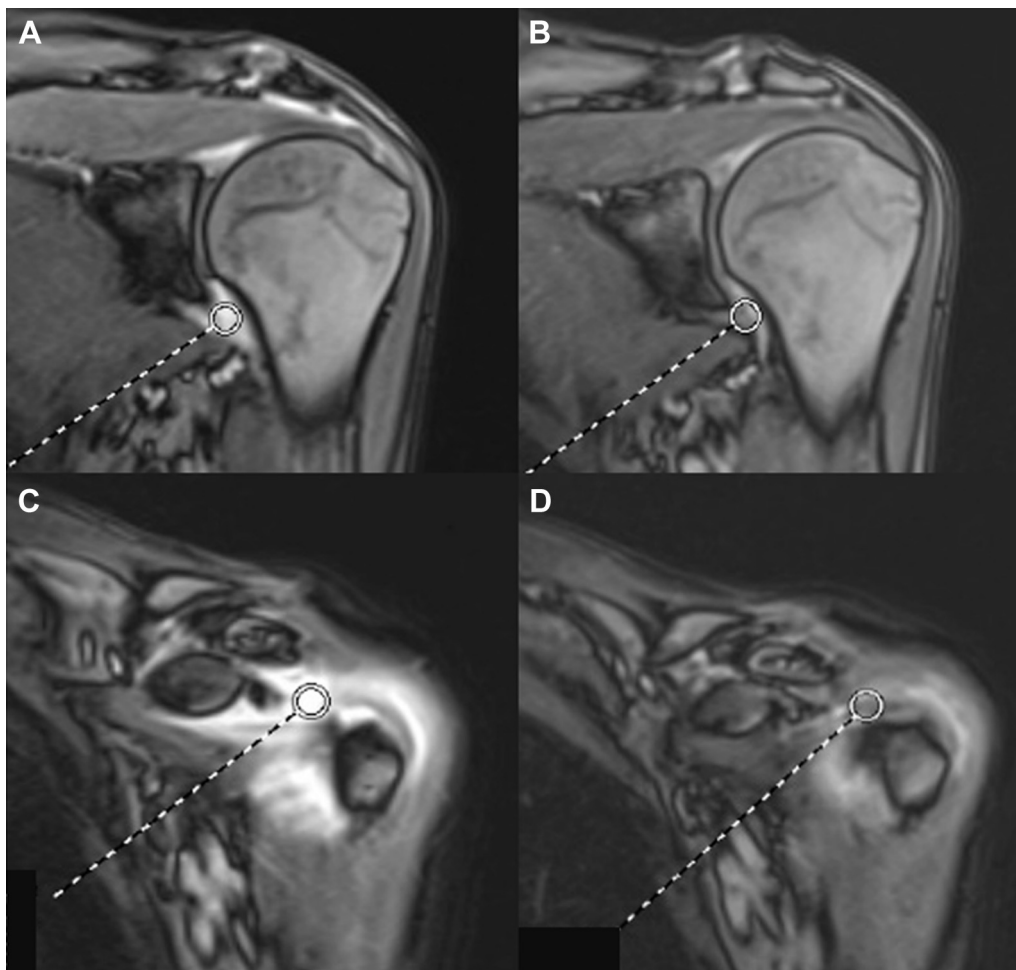


Figure 1 Measurement sites of the AP and RI with dynamic MRI. The measurement sites were determined within the contrast range of the AP and RI by the 0.3-cm² ROI (white circle). (A) is the measured signal intensity within the AP before MUC, (B) is the measured signal intensity within the AP after MUC, (C) is the measured signal intensity within the RI before MUC, and (D) is the measured signal intensity within the RI after MUC. MRI, magnetic resonance imaging; MUC, manipulation under ultrasound-guided cervical nerve root block; AP, axillary pouch; RI, rotator interval; ROI, region of interest.

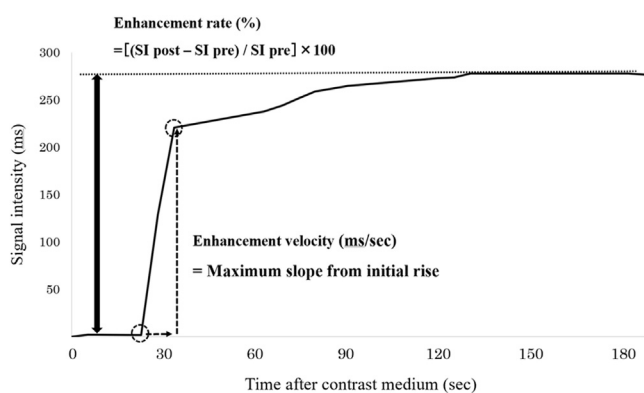


Figure 2 Dynamic MRI kinetic curve of the enhancement site. The increasing rate of the signal intensity (maximum enhancement rate) and the enhancement velocity (initial enhancement speed) were evaluated. MRI, magnetic resonance imaging.

Statistical analysis

Data were expressed as means ± standard deviation. The Wilcoxon signed-rank test was used for comparison. Differences with values of *P* < .05 were considered statistically significant.

Calculations were performed with SPSS 20 software (IBM, Armonk, NY, USA).

Results

Table I shows the patient demographics and clinical characteristics. The burning sign in both AP and RI was detected in all 19 cases using 3D dynamic MRI. The clinical results (NRS score at motion, shoulder ROM, Constant score, and ASES score) of all patients improved after MUC. The NRS improved significantly from 6.1 ± 2.4 preoperatively to 1.1 ± 1.6 at the time of the second dynamic MRI (*P* < .001). Before MUC compared with after MUC, the average values improved for FF from 84° ± 10° to 153° ± 18°, for ER from 0° ± 4° to 55° ± 17°, and for IR from L5 to T10 (all *P* < .001). The preoperative and postoperative ASES score and Constant score were 35 ± 14 and 90 ± 14 and 27 ± 4 and 78 ± 6, respectively (both *P* < .001) (Table II).

The before and after MUC enhancement rate (%) in dynamic MRI SI was 217 ± 51 and 85 ± 36 in the AP and 233 ± 61 and 73 ± 40 in the RI, respectively (both *P* < .001). The before and after MUC enhancement velocities (ms/s) were 902 ± 335 and 203 ± 125 in the AP and 1249 ± 634 and 213 ± 146 in the RI, respectively (both *P* < .001) (Table III).

Table I
Patient demographic and clinical characteristics.

Variables (n = 19)	Values
Age (yr)	55.3 ± 7.1
Sex (female/male)	16/3
Affected side (right/left)	6/13
Pain duration (mo)	5.2 ± 2.1
Interval until dynamic MRI after MUC (mo)	8.2 ± 2.6
Preoperative burning sign (negative/positive)	
AP	0/19
RI	0/19

AP, axillary pouch; RI, rotator interval.
Data are presented as means ± standard deviation.

Table II
Clinical results before and after MUC.

Variables (n = 19)	Before MUC	After MUC	P value
NRS score at motion	6.1 ± 2.4	1.1 ± 1.6	<.001
Range of motion (degrees)			
Forward flexion	84 ± 10 (60-95)	153 ± 18 (110-180)	<.001
External rotation at side	0 ± 4 (-10 to 10)	55 ± 17 (20 to 80)	<.001
Internal rotation	L5 (S-L5)	T10 (L5-T7)	<.001
ASES score	35 ± 14	90 ± 14	<.001
Constant score	27 ± 4	78 ± 6	<.001

MUC, manipulation under ultrasound-guided cervical nerve root block; NRS, numeric rating scale; ASES, American Shoulder and Elbow Surgeons.
Data are presented as means ± standard deviation.

Table III
Semiquantitative evaluation with dynamic MRI before and after MUC.

Variables (n = 19)	Before MUC	After MUC	P value
Increase rate of T1 values (%)			
AP	217 ± 51	85 ± 36	<.001
RI	233 ± 61	173 ± 40	<.001
Enhancement velocity (ms/s)			
AP	902 ± 335	203 ± 125	<.001
RI	1249 ± 634	213 ± 146	<.001

MRI, magnetic resonance imaging; MUC, manipulation under ultrasound-guided cervical nerve root block; AP, axillary pouch; RI, rotator interval.
Data are presented as means ± standard deviation.

Fig. 3 shows 3D dynamic MRI images before and after MUC in a 54-year-old female patient with FS. The burning sign disappeared on 3D dynamic MRI performed six months after MUC. This case also demonstrated the semiquantitative dynamic MRI change at the AP and RI with improvement in clinical results.

All patients enrolled in this study underwent MUC without complications. When the second dynamic MRI was performed, there were no cuff tears, labral tears, capsular tears, or bone bruises found.

Discussion

This study demonstrates the use of dynamic MRI to semiquantitatively evaluate the reduction in abnormal blood flow in patients with FS before and after MUC via examining the enhancement rate of the SI and the enhancement velocity. To our knowledge, this is the first study to use dynamic MRI semiquantitatively to assess the relationship between improvement of the images and clinical outcome in FS after MUC.

We have previously reported the safety and efficacy of MUC in the treatment of FS.¹⁸ The clear benefit of this method is improvement in pain and shoulder ROM as early as 1 week after the procedure.¹⁵ Regarding complications associated with MUC, Horner’s syndrome was reported in one patient in our previous study. However, the symptoms of mild miosis and ptosis resolved after several hours, and the patient returned home on the same day.¹⁵ In this study, no complications, such as fracture, rotator cuff tear, vascular injury, neurological disorder, or pneumothorax, were noted. MRI findings 6 months or more after MUC also did not exhibit any iatrogenic capsular tears, bone bruises, labral tears, or rotator cuff tears.

Sasanuma et al evaluated 3D dynamic MRI findings in patients with FS and found that FS was associated with an abnormal cluster of blood flow and dispersion of contrast medium around the RI and AP.¹⁷ This phenomenon was termed the “burning sign”, and the correlation between this burning sign in the RI and pain score was described. This study demonstrated that the burning sign was a

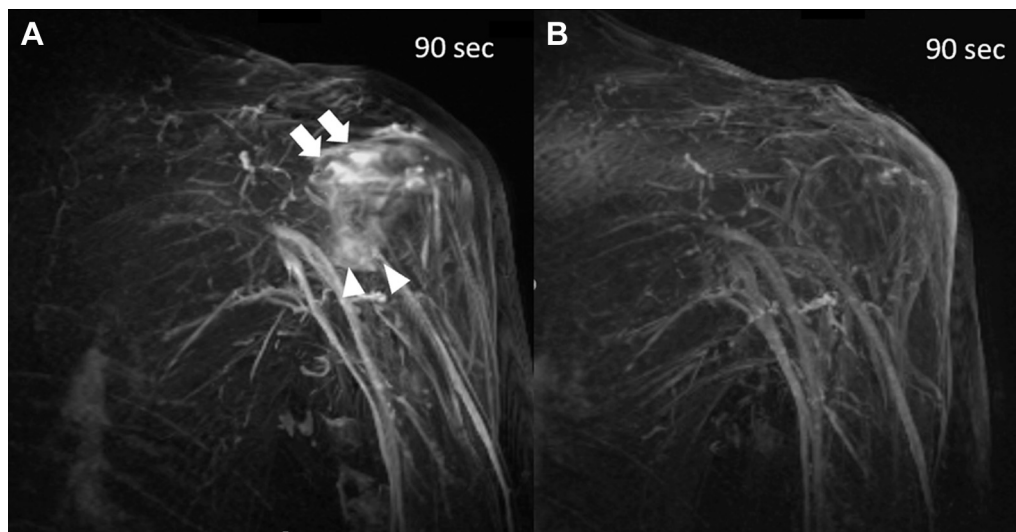


Figure 3 A 54-year-old female patient with idiopathic frozen shoulder of the Left side. (A) Dynamic 3D MRI shows abnormal enhancement (burning sign) at the AP (arrow head) and RI (arrow) before MUC. (B) Dynamic 3D MRI shows the same patient six months after MUC. The burning sign disappeared. Both images are at 90 seconds after the gadolinium intravenous injection (Middle phase). 3D, 3-dimensional; MRI, magnetic resonance imaging; MUC, manipulation under ultrasound-guided cervical nerve root block; AP, axillary pouch; RI, rotator interval.

clear finding on imaging that was likely to be beneficial for the diagnosis of FS.

Tamai et al reported an increase in SI in the glenohumeral joint synovium in patients with FS compared with those of healthy volunteers or patients with subacromial impingement on dynamic MRI.^{20,21} They showed that the increased SI observed in the FS synovium could be reduced by intra-articular injection of corticosteroid or hyaluronate, and the coefficient of enhancement was calculated by setting ROIs on the enhanced area of the dynamic MRI. Against their study, our strong points are to present that the AP and RI have the highest uptake of contrast medium successfully with 3D dynamic MRI and to measure the change of the SI there at a pin point by setting ROIs.

In a study of abnormal blood flow in FS, Okuno et al performed angiography on patients with FS to treat the abnormal vessels by transcatheter arterial embolization.¹² They reported the genesis of neovessels around the AP and RI, and nocturnal pain was immediately diminished after the procedure. Martinez et al also described the effects of transcatheter arterial embolization for 40 patients with FS who were resistant to conservative treatment.¹¹

In addition to using dynamic MRI and angiography, previous studies have reported that specific patterns in positron emission tomography using fluorine-18-fluorodeoxyglucose are helpful to diagnose FS.^{19,22} Won et al reported that the AP and RI may be the main pathologic sites of idiopathic FS based on research using fluorine-18-fluorodeoxyglucose positron emission tomography/computed tomography.²²

These studies suggest that the pathology of FS is closely related to vasculitis at the AP and RI. The outcome of our study, in which clinical signs improved and were accompanied by a decrease in the burning sign, supports these ideas.

To develop the methods used in this study, we referred to the use of dynamic MRI to distinguish malignant breast cancer from benign lesions, as several authors have reported the successful use of dynamic MRI to determine therapeutic strategies for breast tumors.^{3,10,23} Yang et al demonstrated that a kinetic modeling curve using a contrast pattern showed higher sensitivity, specificity, and positive and negative predictive values than the intensity curve method when using dynamic MRI in breast lesion classification.²³

In this study, we evaluated not only the SI at the AP and RI but also the contrast speed from the kinetic curve. However, we did not use contrast strength or speed to determine the prognosis or severity of FS. In the future, semiquantitative evaluation of FS using dynamic MRI could be used to classify FS and determine prognosis.

There are several limitations to our study. First, the sample size was small, and the follow-up period was short, so a prospective study with a larger sample size and a longer follow-up is necessary. Second, there was no comparison group of patients with idiopathic FS who did not undergo MUC, and the natural course of idiopathic FS in dynamic MRI images is unknown. Third, patients with diabetes mellitus were excluded only by asking about their medical history, so it is possible that diabetic stiff shoulder may have been concealed. Finally, we performed the second dynamic MRI 6 months or more after MUC, so it is possible that had the dynamic MRI been performed earlier, the burning sign may have disappeared or decreased sooner than 6 months after MUC. In the future, more detailed monitoring of dynamic MRI findings and clinical symptoms over time after the MUC is needed.

Conclusions

The burning sign was observed at the AP and RI on dynamic MRI in all patients with FS, and dynamic MRI semiquantitatively demonstrated a reduction in the burning sign with improvement of

clinical symptoms in patients after MUC. This method of using dynamic MRI to evaluate FS may help to diagnose FS and evaluate the effects of therapy. Furthermore, our findings suggest that there is an association between the burning sign and the pathology of FS.

Disclaimers:

Funding: The authors did not receive and will not receive any benefits and funding from any commercial party related directly or indirectly to the subject of this article.

Conflicts of interest: The author, their immediate family, and any research foundation with which they are affiliated have not received any financial payments or other benefits from any commercial entity related to the subject of this article.

Acknowledgments

The authors thank Leonie McKinlay, DVM, from Edanz (<https://jp.edanz.com/ac>) for editing a draft of this manuscript.

References

- Andersen NH, Sojbjerg JO, Johannsen HV, Sneppen O. Frozen shoulder: arthroscopy and manipulation under general anesthesia and early passive motion. *J Shoulder Elbow Surg* 1998;7:218-22.
- Ando A, Hamada J, Hagiwara Y, Sekiguchi T, Koide M, Itoi E. Short-term clinical results of manipulation under ultrasound guided brachial plexus block in patients with idiopathic frozen shoulder and diabetic secondary frozen shoulder. *Open Orthop J* 2018;12:99e104. <https://doi.org/10.2174/1874325001812010099>.
- Cheng L, Li X. Breast magnetic resonance imaging: kinetic curve assessment. *Gland Surg* 2013;2:50-3. <https://doi.org/10.3978/j.issn.2227-684X.2013.02.04>.
- Cho CH, Bae KC, Kim DH. Treatment Strategy for frozen shoulder. *Clin Orthop Surg* 2019;11:249-57. <https://doi.org/10.4055/cios.2019.11.3.249>.
- Codman EA. *The shoulder: Rupture of the supraspinatus tendon and other lesions in or about the subacromial bursa*. Boston: Thomas Todd Co; 1934.
- Farrell CM, Sperling JW, Cofield RH. Manipulation for frozen shoulder: long-term results. *J Shoulder Elbow Surg* 2005;14:480-4. <https://doi.org/10.1016/j.jse.2005.02.012>.
- Hagiwara Y, Kanazawa K, Ando A, Sekiguchi T, Koide M, Yabe Y, et al. Effects of joint capsular release on range of motion in patients with frozen shoulder. *J Shoulder Elbow Surg* 2020;29:1836-42. <https://doi.org/10.1016/j.jse.2020.01.085>.
- Hand C, Clipsham K, Rees JL, Carr AJ. Long-term outcome of frozen shoulder. *J Shoulder Elbow Surg* 2008;17:231-6. <https://doi.org/10.1016/j.jse.2007.05.009>.
- Hsu JE, Anakwenze OA, Warrender WJ, Abboud JA. Current review of adhesive capsulitis. *J Shoulder Elbow Surg* 2011;20:502e14. <https://doi.org/10.1016/j.jse.2010.08.023>.
- Khoulil RH, Macura KJ, Jacobs MA, Khalil TH, Kamel IR, Dwyer A, et al. Dynamic contrast-enhanced MRI of the breast: quantitative method for kinetic curve type assessment. *AJR Am J Roentgenol* 2009;193:W295-300. <https://doi.org/10.2214/AJR.09.2483>.
- Martínez AM, Baldi S, Alonso-BurgosA, Lopez R, Vallejo-Pascual ME, Marcos MT, et al. Mid-term results of transcatheter arterial embolization for adhesive capsulitis resistant to conservative treatment. *Cardiovasc Intervent Radiol* 2021;44:443-51. <https://doi.org/10.1007/s00270-020-02682-4>.
- Okuno Y, Oguro S, Iwamoto W, Miyamoto T, Ikegami H, Matsumura N. Short-term results of transcatheter arterial embolization for abnormal neovessels in patients with adhesive capsulitis: a pilot study. *J Shoulder Elbow Surg* 2014;23:e199-206. <https://doi.org/10.1016/j.jse.2013.12.014>.
- Paul MR, Jennie N, Christopher PR. Randomized controlled trial of supervised physiotherapy versus a home exercise program after hydrodilatation for the management of primary frozen shoulder. *J Shoulder Elbow Surg* 2017;26:757-65. <https://doi.org/10.1016/j.jse.2017.01.012>.
- Russell S, Jariwala A, Conlon R, Selve J, Richards J, Walton M. A blinded, randomized, controlled trial assessing conservative management strategies for frozen shoulder. *J Shoulder Elbow Surg* 2014;23:500-7. <https://doi.org/10.1016/j.jse.2013.12.026>.
- Saito T, Sasanuma H, Iijima Y, Kanaya Y, Saito T, Watanabe H, et al. Short term clinical results of frozen shoulder treated with shoulder manipulation under ultrasound-guided cervical nerve root block at outpatient setting: a case series. *J Orthop Sci* 2017;22:275e80. <https://doi.org/10.1016/j.jos.2016.11.007>.
- Saito T, Sugimoto H, Sasanuma H, Iijima Y, Kanaya Y, Fukushima T, et al. The course and clinical impact of articular magnetic resonance imaging findings 6 months after shoulder manipulation under ultrasound-guided cervical nerve root block for frozen shoulder. *J Shoulder Elbow Surg Open Access* 2019;18:21-4. <https://doi.org/10.1016/j.jses.2018.11.001>.

17. Sasanuma H, Sugimoto H, Fujita A, Kanaya Y, Iijima Y, Saito T, et al. Characteristics of dynamic magnetic resonance imaging of idiopathic severe frozen shoulder. *J Shoulder Elbow Surg* 2017;26:e52-7. <https://doi.org/10.1016/j.jse.2016.06.003>.
18. Sasanuma H, Sugimoto H, Kanaya Y, Iijima Y, Saito T, Saito T, et al. Magnetic resonance imaging and short-term clinical results of severe frozen shoulder treated with manipulation under ultrasound-guided cervical nerve root block. *J Shoulder Elbow Surg* 2016;25:e13-20. <https://doi.org/10.1016/j.jse.2015.06.019>.
19. Sridharan R, Engle MP, Garg N, Wei W, Amini B. Focal uptake at the rotator interval or inferior capsule of shoulder on 18 F-FDG PET/CT is associated with adhesive capsulitis. *Skeletal Radiol* 2017;46:533-8. <https://doi.org/10.1007/s00256-017-2587-8>.
20. Tamai K, Yamato M. Abnormal synovium in the frozen shoulder. A preliminary report with dynamic magnetic resonance imaging. *J Shoulder Elbow Surg* 1997;6:534-43.
21. Tamai K, Mashitori M, Ohno W, Hamada J, Sakai H, Saotome K. Synovial response to intraarticular injections of hyaluronate in frozen shoulder: a quantitative assessment with dynamic magnetic resonance imaging. *J Orthop Sci* 2004;9:230. <https://doi.org/10.1007/s00776-004-0766-7>.
22. Won KS, Kim DH, Sung DH, Song BI, Kim HW, Song KS, et al. Clinical correlation of metabolic parameters on (18)F-FDG PET/CT in idiopathic frozen shoulder. *Ann Nucl Med* 2017;31:211-7. <https://doi.org/10.1007/s12149-016-1147-y>.
23. Yang SN, Li FJ, Chen JM, Zhang G, Liao YH, et al. Kinetic curve type Assessment for classification of breast lesions using dynamic contrast-enhanced MR imaging. *PLoS One* 2016;7:e0152827. <https://doi.org/10.1371/journal.pone.0152827>.